Autorotation design and simulation for a small-scale helicopter

Giulio Avanzini, giulio.avanzini@unisalento.it, University of Salento (Italy)

Emanuele L. de Angelis, emanuele.deangelis4@unibo.it, University of Bologna (Italy)

Daniele Fattizzo, daniele.fattizzo2@unibo.it, University of Bologna (Italy)

Fabrizio Giulietti, fabrizio.giulietti@unibo.it, University of Bologna (Italy)

Abstract

Safety of manned and unmanned aircraft is strictly related to the capability of managing emergency situations. In the case of helicopter engine failure, the autorotation manoeuvre represents a valid possibility for a safe emergency landing.

Such manoeuvre is made of two different main phases: 1) the steady descent, where the rotor angular rate is kept in a proper range and the helicopter descends with constant velocity, and 2) the final flare, where the kinetic energy stored in the main rotor is used to generate a braking force, so to reduce the vertical velocity to a minimum value.

For a manned piloted helicopter, experience and piloting skills of the pilot are mandatory for performing a safe emergency landing. For unmanned rotorcraft, since the remote pilot does not have the direct perception of linear accelerations and attitude motion, the remote autorotation is indeed an extremely hazardous task.

For this reason, there is a significant interest in the design of a control algorithms allowing a remotely piloted helicopter to automatically perform the autorotation manoeuvre, which is a crucial feature for all missions over populated areas and/or for all aircraft carrying expensive payloads.

In this paper, a preliminary investigation on steady descent conditions in autorotation, and a first design of a complete autorotation maneuver has been made through a model-based design approach. Also, a closed loop control system has been developed, to perform the two main phases of autorotation. Simulations results show the suitability of the proposed approach for a wide range of initial conditions (altitude and advancing velocity).

NOMENCLATURE

a_0	Rotor coning angle (rad)
a_1	Longitudinal rotor tip path plane deflection angle in rotor-hub system (rad)
A_{1c}	Lateral cyclic pitch measured from hub plane in Wind-Hub axes system(rad)
A_{1s}	Lateral cyclic pitch measured from hub plane in Hub-Body axes system(rad)
b_1	Lateral rotor tip path plane deflection angle in rotor-hub system (rad)
B_{1c}	Longitudinal cyclic pitch measured from hub plane in Wind-Hub axes system(rad)
B_{1s}	Longitudinal cyclic pitch measured from hub plane in Hub-Body axes system(rad)
$\widetilde{D}$	Damping matrix for flapping
e	Flapping hinge offset (m)
$\tilde{f}$	Forcing function for flapping
$\widetilde{K}$	Stiffness matrix for flapping
K_1	Pitch-flap coupling ratio
M_β	Blade weight moment about the flapping hinge (N·m)
M_{tot}	Total mass (kg)
U_T	Blade element velocity on the hub plane (m/s)
U_P	Blade element velocity normal to the hub plane (m/s)

$\mathbf{I} = \begin{bmatrix} I_{xx} & I_{xy} & I_{xz} \\ I_{yx} & I_{yy} & I_{yz} \\ I_{zx} & I_{zy} & I_{zz} \end{bmatrix}$	Inertia tensor (kg/m^2)
$\mathbf{F}_{(\cdot)} = [X \quad Y \quad Z]^T$	Forces vector (N)
$\boldsymbol{M}_{(\cdot)} = [L \quad M \quad N]^T$	Moments vector (Nm)
$\mathbf{V}_{(\cdot)} = [u \quad v \quad w]^T$	Linear velocity vector (m/s)
$\boldsymbol{\omega}_{(\cdot)} = [p \quad q \quad r]^T$	Angular velocity vector (rad/s)
β	Blade flapping (rad)
ε	Hinge offset ratio
μ	Advance ratio
λ	Inflow ratio
ϕ, θ, ψ	Roll, pitch, yaw Euler angles (rad)
θ_0	Blade root collective pitch (rad)
Ω	Rotor angular velocity (rad/s)
	Subscripts
b	Body frame
cl	Clockwise
ccl	Counter-clockwise
E	Earth fixed NED frame
e	Equilibrium condition
fus	Fuselage
h	Hub-Body frame
LV	Local-Vertical frame
mr	Main rotor
sd	Steady descent
w	Wind-Hub frame
	Superscripts
a	Aerodynamic
e	External
g	Gravitational

1. INTRODUCTION

Engine failure represents one of the most critical situations for any aircraft. For a helicopter, the main way for a safe emergency landing, is represented by autorotation. This maneuver has two main phases: in the first one it is necessary to keep the rotor at a constant rotation speed by exploiting the descent flow to minimize the aerodynamic torque; in the second phase, when the altitude reached is adequate, it is instead necessary to exploit the saved rotor energy, to produce braking and touch the ground at minimum speed.

For manned helicopters, the ability of the pilot is of primary importance for the success of the maneuver and therefore for the safety of the pilot himself. Moreover a good landing avoids or minimizes damage to the aircraft reducing economic losses. For an unmanned aerial vehicle, danger for people and economic loss is usually reduced and the possibility of an emergency landing maneuver is often neglected. A shot-down system is more often implemented.

However, there are conditions where costs and risks increase, especially in the case of important payloads which should be saved. An increasing use of unmanned systems in urban or work environment is also leading to deeper interest and research in this field.

In autorotation the main task is to reduce sink rate to minimum value minimizing the impact velocity and therefore damages. The optimal trajectory to minimize touch down velocity has been evaluated in [1] considering a very simple model of the vertical dynamics of the helicopter. Similar optimal approach, but with a more complex cost function and dynamics model have been considered in [2] and in [3] where, in the latter, an optimal trajectory and control system for the tracking have been evaluated.

Scope of this paper is to give a preliminary analysis on the autorotation and to design a suitable autorotation maneuver and a simple autonomous control system able to perform it.

In section 2 the dynamic model of the helicopter, and the design of a suitable autorotation maneuver is described. Section 3 shows main simulations set-up and results.

2. MATHEMATICAL MODELLING

2.1. Aircraft dynamics

An overview of main equations and assumptions for the dynamic model of the Helicopter is here given.

2.1.1. Reference frames and coordinate transformation

Six orthogonal reference frames are introduced: Hub-Wind; Hub-Body, Body, Aircraft and Local Wind. In particular, the term "Hub" means that the origin of the coordinate system is at the main rotor hub centre.

The terms "Wind" and "Body" indicate where the three axes point.

1. An Earth-fixed North–East-Down frame, $\mathbb{F}_E = \{O;\ \boldsymbol{x}_E, \boldsymbol{y}_E, \boldsymbol{z}_E\}$. This frame is inertial under the assumption of flat and non-rotating Earth.
2. Hub Wind Frame $\mathbb{F}_{hw} = \{H;\ \boldsymbol{x}_{hw}, \boldsymbol{y}_{hw}, \boldsymbol{z}_{hw}\}$. This frame is used in calculation of rotor forces and moments. Its origin is the rotor hub. $\mathbf{z}_{hw}$ axis is aligned with the rotor shaft, pointing upward. $\mathbf{x}_{hw}$ axis (horizontal) is aligned with the component of relative wind normal to the shaft axis. $\mathbf{y}_{hw}$ axis completes the right-handed orthogonal set.
3. Hub Body Frame $\mathbb{F}_{hb} = \{H;\ \boldsymbol{x}_{hb}, \boldsymbol{y}_{hb}, \boldsymbol{z}_{hb}\}$. $\mathbf{z}_{hb}$ axis is aligned with rotor shaft, pointing upward. This system coincides with the hub-wind system when the sideslip β_w is zero.
4. Body Fixed Frame $\mathbb{F}_b = \{P;\ \boldsymbol{x}_b, \boldsymbol{y}_b, \boldsymbol{z}_b\}$. Origin is located at the centre of gravity of the rotorcraft. $\mathbf{x}_b$ axis points in forward direction, it's aligned with the longitudinal axis of the vehicle; $\mathbf{z}_b$ is perpendicular to $\mathbf{x}_b$ in the longitudinal plane pointing downward, and $\mathbf{y}_b$ axis completes the right-hand system. All forces and moments used in the body equations of motion are expressed relative to this system.
5. Wind Frame $\mathbb{F}_w = \{R;\ \boldsymbol{x}_w, \boldsymbol{y}_w, \boldsymbol{z}_w\}$. These axes are used to calculate lift and drag forces on the fuselage. The origin is in the fuselage pressure centre.
6. Local Vertical Frame $\mathbb{F}_{LV} = \{P;\ \boldsymbol{x}_{LV}, \boldsymbol{y}_{LV}, \boldsymbol{z}_{LV}\}$. Origin is at the centre of gravity and axes are parallel to the inertial frame.

Rotor flapping dynamics assessment and rotor forces and moments calculation require linear and angular velocity vectors and acceleration vector as expressed in the Hub-Body system and the angle of sideslip at the hub. The cyclic pitch is also requested in Hub-Wind system.
In this respect, the velocity vector at the hub is written as follows:

(1) $$\boldsymbol{V_h} = \boldsymbol{\Pi_{hb}}[\boldsymbol{V_b} + \boldsymbol{\omega_b} \times \boldsymbol{r_b}]$$

whereas angular velocity and acceleration are given by:

(2) $$\boldsymbol{\omega_h} = \boldsymbol{\Pi_{hb}}\boldsymbol{\omega_b}$$

(3) $$\dot{\boldsymbol{\omega}}_{\boldsymbol{h}} = \boldsymbol{\Pi_{hb}}\dot{\boldsymbol{\omega}}_{\boldsymbol{b}}$$

where $\boldsymbol{\Pi_{hb}}$ is the rotational matrix from Body to Hub-Body system. Since rotor shafts is tilted in XZ plane with an angle i_s, Π_{hb} is written as:

(4) $$\boldsymbol{\Pi_{hb}} = \begin{bmatrix} \cos i_s & 0 & \sin i_s \\ 0 & 1 & 0 \\ -\sin i_s & 0 & \cos i_s \end{bmatrix}$$

Calculated Wind-Hub system components are then rotated to be implemented into the 6-DOF equations of motion:

(5) $$\begin{bmatrix}(\cdot)_x \\ (\cdot)_y\end{bmatrix}_{wh} = \begin{bmatrix}\cos\beta_w & \sin\beta_w \\ -\sin\beta_w & \cos\beta\_w\end{bmatrix}\begin{bmatrix}(\cdot)_x \\ (\cdot)_y\end{bmatrix}_{hb}$$

Where

(6) $$\beta_w = \sin^{-1}\frac{v_h}{\sqrt{v_h^2+u_h^2}}$$

is the sideslip angle.

2.1.2. Dynamic model

Helicopter dynamics model considers the following state vector:

(7) $$\boldsymbol{x} = [\boldsymbol{V_b}; \boldsymbol{\omega_b}; \boldsymbol{a}; \lambda_i; \Omega]$$

and command vector:

(8) $$\boldsymbol{u} = [\theta_0; A_{1s}; B_{1s}; \theta_{tr}]$$

Where $\boldsymbol{V_b} = [u\ v\ w]'$ and $\boldsymbol{\omega_b} = [p\ q\ r]'$ are the rigid body 6dofs in the body reference frame, $\boldsymbol{a} = [a_0\ a_1\ b_1]'$ is the vector of flapping angles, $\lambda_i = \frac{V_i}{\Omega R}$ is the inflow ratio due to rotor thrust induced velocity, and Ω is the main rotor angular speed. The command vector components are: the collective pitch θ_0, the lateral and longitudinal pitch angle in the Hub-body frame A_{1s}, B_{1s}, and the tail rotor pitch θ_{tr}.

The equations involved are:

- Equations of motions in body reference frame

(9) $$\begin{cases} \dot{\boldsymbol{V}}_{\boldsymbol{b}} = -\boldsymbol{\omega_b} \times \boldsymbol{V_b} + \boldsymbol{F_b}/M_{tot} \\ \dot{\boldsymbol{\omega}}_{\boldsymbol{b}} = \boldsymbol{I}^{-1}[-\boldsymbol{\omega_b} \times (\boldsymbol{I}\boldsymbol{\omega_b}) + \boldsymbol{M_b}] \end{cases}$$

Where forces and moments are the sum of aerodynamic and gravitational effects for all the helicopter subsystems (main rotor, tail rotor, fuselage).

(10) $$\begin{cases} \boldsymbol{F_b} = \boldsymbol{F_{mr}^a} + \boldsymbol{F_{tr}^a} + \boldsymbol{F_{fus}^a} + \boldsymbol{W} \\ \boldsymbol{M_b} = \boldsymbol{M_{mr}^a} + \boldsymbol{M_{tr}^a} + \boldsymbol{M_{fus}^a} \end{cases}$$

- Flapping dynamics equation

(11) $$\ddot{\boldsymbol{a}} = -\widetilde{\boldsymbol{D}}\dot{\boldsymbol{a}} - \widetilde{\boldsymbol{K}}\boldsymbol{a} + \tilde{\boldsymbol{f}}$$

Where the components of the flapping vector $\boldsymbol{a}$ represent the time variant coefficients of the tip path-plane flapping equation:

(12) $$\beta(t,\psi) = a_0(t) + a_1(t)\cdot\cos\psi + b_1(t)\cdot\sin\psi$$

With $\beta(\psi,t)$ flapping angle of the blade having an azimuth angle ψ. The flapping model is derived in [4].

- Inflow dynamics equation

(13) $$\dot{\lambda}_i = \frac{3\pi}{4}\left\{\frac{C_t}{2} - \lambda_i\sqrt{\mu^2+\lambda^2}\right\}$$

Where C_t is the main rotor thrust coefficient, $\mu = \frac{\sqrt{u_h^2+v_h^2}}{\Omega R}$ is the advance ratio with respect to hub-body frame and $\lambda = \frac{w_h}{\Omega R} - \lambda_i$ is the total inflow ratio.

Here a uniform dynamic model, derived from [5], has been chosen to simplify analytical evaluation of the main rotor forces and moments.

- Rotor dynamics equation

Calling I_{mr} and I_{tr} the rotational inertia moments of the main and tail rotor, and τ the transmission ratio between main and tail rotor rotational speeds, the kinetic energy of the rotors is:

$$T_{rotors} = \frac{1}{2}I_{mr}\Omega_{mr}^2 + \frac{1}{2}I_{tr}\Omega_{tr}^2 = \frac{1}{2}(I_{mr}+\tau^2 I_{tr})\Omega_{mr}^2$$

The energy conservation equation for the system Engine-Rotors is given by:

$$\frac{dT_{rotors}}{dt} = P_e - P_{rotors}$$

Thus

$$(I_{mr}+\tau^2 I_{tr})\Omega_{mr}\dot{\Omega}_{mr} = P_e - P_{rotors}$$

Where P_e is the power provided by the engine and P_{rotors} is the power absorbed by the rotors which can be written as:

$$P_{rotors} = Q_{mr}\cdot\Omega_{mr} + Q_{tr}\cdot\Omega_{tr} = (Q_{mr}+\tau Q_{tr})\Omega_{mr}$$

When the Engine is on, a control system keeps rotational speeds constant varying the engine power. In the Engine off case, as in autorotation, the term P_e is zero and the equation becomes:

$$(I_{mr}+\tau^2 I_{tr})\Omega_{mr}\dot{\Omega}_{mr} = -(Q_{mr}+\tau Q_{tr})\Omega_{mr}$$

Which gives:

(14) $$\dot{\Omega}_{mr} = -\frac{(Q_{mr}+\tau Q_{tr})}{I_{mr}+\tau^2 I_{tr}} \cong -\frac{Q_{mr}}{I_{mr}}$$

Where tail rotor influence has been neglected.

All the previous equations are nonlinear with respect to the state vector, and they are all coupled.

2.1.3. Attitude Kinematics

The attitude of the rotorcraft is expressed by means of Euler Angles $[\Phi\ \Theta\ \Psi]'$ which varies in time as a function of $\boldsymbol{\omega_b}$ as follows:

(15) $$\begin{bmatrix}\dot{\phi}\\ \dot{\Theta}\\ \dot{\Psi}\end{bmatrix} = \begin{bmatrix}1 & \sin\phi\tan\Theta & \cos\phi\tan\Theta\\ 0 & \cos\phi & -\sin\phi\\ 0 & \frac{\sin\phi}{\cos\Theta} & \frac{\cos\phi}{\cos\Theta}\end{bmatrix}\boldsymbol{\omega_b}$$

The velocities in Earth inertial axes are written as function of Euler angles and velocities in body frame:

(16) $$\begin{bmatrix}\dot{x}\\ \dot{y}\\ \dot{z}\end{bmatrix} = \boldsymbol{\Pi_{Eb}}\begin{bmatrix}u\\ v\\ w\end{bmatrix}$$

(17) $$\boldsymbol{\Pi_{Eb}} = \begin{bmatrix}\mathrm{c}\Theta c\Psi & \mathrm{s}\phi s\Theta\mathrm{c}\Psi - \mathrm{c}\phi s\Psi & \mathrm{c}\phi s\Theta\mathrm{c}\Psi + \mathrm{s}\phi s\Psi\\ \mathrm{c}\Theta\mathrm{s}\Psi & \mathrm{s}\phi s\Theta\mathrm{s}\Psi + \mathrm{c}\phi c\Psi & \mathrm{c}\phi s\Theta\mathrm{s}\Psi - \mathrm{s}\phi c\Psi\\ -s\Theta & \mathrm{s}\Phi c\Theta & \mathrm{c}\phi c\Theta\end{bmatrix}$$

2.1.4. Main rotor

The hinge-less rotor is modelled as a teetering rotor where an equivalent rotor flapping stiffness K_β is introduced as a correction of the ideal teetering model. Flapping dynamics is approximated using a tip-path-plane representation. The following assumptions are introduced:

1. Rotor blade is rigid in bending and torsion;
2. Linear blade twist;
3. Flapping and inflow angles are assumed small, the analysis is based on a simple strip theory;
4. Only effects due to angular acceleration $\dot{p}$ and $\dot{q}$, angular velocity p, q and the normal acceleration of the aircraft motion are considered to calculate blade flapping;
5. Compressibility and stall effects are not considered;
6. Reversed flow region is not considered;
7. The inflow is assumed to be uniform;
8. The tip loss factor is assumed to be 1;

9. Blade flapping is approximated by the first harmonic terms with time-varying coefficients as in equation (12).

According to blade flapping approximation in equation (12), a_0 is treated as a pre-set constant and coefficients $a_1(t)$ and $b_1(t)$ can be evaluated considering $\dot{a}_0 = \ddot{a}_0 = 0$ in equation (11).

The analytical evaluation of main rotor forces and moments is done using the blade-element theory. The total force on a blade having a ψ azimuth is obtained integrating the force on the blade element over the rotor radius. Then the integration with respect to the azimuth $\psi = [0; 2\pi]$ gives the mean force of the blade over a complete rotation around the shaft. Equations are first obtained in the Wind-Hub coordinate system and then transformed into Body system. Complete derivation of Main rotor forces is given in [6] where the only difference with respect to our assumptions is that in [6] a static-uniform inflow is used, while we adopted a dynamic-uniform inflow.

2.1.5. Clockwise correction factors

The equations derived in [4] [6] [7] are valid for a counter-clock-wise rotor. When the rotation is clock-wise a correction factor needs to be add Introducing a parameter χ which value is equal to 1 when rotor is counter-clockwise; -1 otherwise. Resulting equations are given as follows:

$$\begin{aligned} \boldsymbol{V}_{cl} &= \Pi_1 \boldsymbol{V}_{ccl} \\ \boldsymbol{\omega}_{cl} &= \Pi_2 \boldsymbol{\omega}_{ccl} \\ \boldsymbol{F}_{cl} &= \Pi_1 \boldsymbol{F}_{ccl} \\ \boldsymbol{M}_{cl} &= \Pi_2 \boldsymbol{M}_{ccl} \\ [\theta_0\ A_{1s}\ B_{1s}]'_{cl} &= \Pi_1 [\theta_0\ A_{1s}\ B_{1s}]'_{ccl} \end{aligned} \tag{18}$$

provided $\Pi_1 = \begin{bmatrix} 1 & 0 & 0 \\ 0 & \chi & 0 \\ 0 & 0 & 1 \end{bmatrix}$, $\Pi_2 = \begin{bmatrix} \chi & 0 & 0 \\ 0 & 1 & 0 \\ 0 & 0 & \chi \end{bmatrix}$

2.1.6. Tail rotor

Tail rotor is modelled as in [7], where flapping dynamics is ignored and a steady state solution for flapping angles, Forces and Moments is considered. The inflow ratio is here static and uniform and it is obtained as a steady state of a Pitt-Peters model:

$$\lambda_{tr} = -\frac{v_{tr}}{\Omega_{tr} R_{tr}} - \frac{C_{t,tr}}{2\sqrt{\mu_{tr}^2 + \lambda_{tr}^2}} \tag{19}$$

This equation needs to be solved with a Newton-Ralphson method for every time step.

2.1.7. Fuselage

The Fuselage Forces and Moments are evaluated as a function of the angle of attack and the sideslip angle. Aerodynamic coefficients are obtained with estimated look-up tables. Main equations are:

$$\begin{aligned} \boldsymbol{V}_{\boldsymbol{fus}} &= \boldsymbol{V}_{\boldsymbol{b}} + \boldsymbol{\omega}_{\boldsymbol{b}} \times \boldsymbol{r}_{\boldsymbol{fus}} \\ \alpha_{fus} &= \operatorname{atan} \frac{w_{fus}}{u_{fus}} \\ \beta_{fus} &= \operatorname{asin} \frac{v_{fus}}{|V_{fus}|} \\ D &= \frac{1}{2} \rho |V_{fus}|^2 S_{ref} C_D(\alpha, \beta) \\ Y &= \frac{1}{2} \rho |V_{fus}|^2 S_{ref} C_Y(\alpha, \beta) \\ L &= \frac{1}{2} \rho |V_{fus}|^2 S_{ref} C_L(\alpha, \beta) \end{aligned} \tag{20}$$

$$\boldsymbol{F}_{\boldsymbol{fus}}^{\boldsymbol{a}} = \begin{bmatrix} -\cos\alpha_{fus}\cos\beta_{fus} & -\sin\alpha_{fus}\sin\beta_{fus} & \sin\alpha_{fus} \\ -\sin\beta_{fus} & \cos\beta_{fus} & 0 \\ -\sin\alpha_{fus}\cos\beta_{fus} & -\sin\alpha_{fus}\sin\beta_{fus} & \cos\alpha_{fus} \end{bmatrix} \begin{pmatrix} D \\ Y \\ L \end{pmatrix}$$

$$\boldsymbol{M}_{\boldsymbol{fus}}^{\boldsymbol{a}} = \boldsymbol{r}_{\boldsymbol{fus}} \times \boldsymbol{F}_{\boldsymbol{fus}}^{\boldsymbol{a}}$$

Where $\boldsymbol{r}_{\boldsymbol{fus}}$ is the position of the fuselage pressure center with respect to gravity center of the rotorcraft.

2.1.8. Gravitational force

Helicopter weight force in body axes is written as:

$$\boldsymbol{W}_{\boldsymbol{b}} = Mtot \cdot g \cdot \begin{bmatrix} \sin\Theta \\ \sin\phi\cos\Theta \\ \cos\phi\cos\Theta \end{bmatrix} \tag{21}$$

2.2. Design of a suitable autorotation maneuver

Helicopter autorotation is a safe landing maneuver which needs to be performed in the case of total power loss. It can be divided in two main phases: the steady descent and the flare.

When the Engine is Off the rotor aerodynamic torque is no more equilibrated by the engine and the rotor speed starts decreasing. This makes the thrust decreasing, and the helicopter starts a descent. The impinging flow can reduce aerodynamic torque keeping a certain level of rotor speed. In this case the rotor is in wind-mill-state and provides a residual thrust which contrast the gravitational force reducing the sink rate. A steady descent is then possible

calibrating collective pitch such that constant rpms are kept. The value of this rotational speed is a function of the sink rate and needs to be optimized to keep a sufficient level of rotational energy to perform the final flare. This last phase is done to reduce sink rate and advancing velocity to minimum values at touch down, exploiting all the residual energy to produce a braking force.

Decreasing rotor speed under minimum acceptable level during the steady descent prevents the rotor from generating the thrust necessary for a safe landing. Acceptable values for touch down velocities and final attitude are set to:

$$\begin{cases} u_{E_{max,TD}} = 0.5\ m/s \\ v_{E_{max,TD}} = 0.5\ m/s \\ w_{E_{max,TD}} = 0.25\ m/s \\ -10° < \Phi_{\mathrm{TD}} < 10° \\ -10° < \Theta_{\mathrm{TD}} < 10° \end{cases} \tag{22}$$

In this work no constraints are considered on the helicopter final position. Then an infinite extended landing field is assumed, and a pure longitudinal and ideally rectilinear maneuver is modelled.

The approach adopted here for the design of a suitable maneuver, is to divide the two main phases, evaluate all the possible steady descent conditions, and to design a simple and effective strategy for the flare.

2.2.1. Steady descent

All the possible steady descent conditions have been evaluated considering the whole mathematical model and calculating equilibrium conditions for imposed advancing velocities u_e and sink rates w_e:

Imposed conditions:

$$\begin{cases} \boldsymbol{V_E} = [u_E\ 0\ w_E]' \rightarrow \boldsymbol{V_b} = \boldsymbol{\Pi_{bE}}(\Phi, \Theta) \cdot \boldsymbol{V_E} \\ \boldsymbol{\omega_b} = [0\ 0\ 0]' \\ \dot{\boldsymbol{a}} = [0\ 0\ 0]' \end{cases} \tag{23}$$

Resulting problem:

$$\begin{cases} \dot{\boldsymbol{V}}_{\boldsymbol{b}} = -\boldsymbol{\omega_b} \times \boldsymbol{V_b} + \frac{\boldsymbol{F_b}}{M_{tot}} = \boldsymbol{0} \\ \dot{\boldsymbol{\omega}}_{\boldsymbol{b}} = \boldsymbol{I}^{-1}[-\boldsymbol{\omega_b} \times (\boldsymbol{I\omega_b}) + \boldsymbol{M_b}] = \boldsymbol{0} \\ \ddot{\boldsymbol{a}} = -\widetilde{\boldsymbol{D}}\dot{\boldsymbol{a}} - \widetilde{\boldsymbol{K}}\boldsymbol{a} + \tilde{\boldsymbol{f}} = \boldsymbol{0} \\ \dot{\lambda}_i = \frac{3\pi}{4}\left\{\frac{C_t}{2} - \lambda_i\sqrt{\mu^2 + \lambda^2}\right\} = 0 \\ \dot{\Omega} = -\frac{Q_{mr}}{I_{mr}} = 0 \end{cases} \rightarrow \tag{24}$$

$$\begin{cases} \boldsymbol{F_b}(\boldsymbol{V_E}, \boldsymbol{a}, \boldsymbol{u}, \Phi, \Theta, \lambda, \Omega) = \boldsymbol{0} \\ \boldsymbol{M_b}(\boldsymbol{V_E}, \boldsymbol{a}, \boldsymbol{u}, \Phi, \Theta, \lambda, \Omega) = \boldsymbol{0} \\ \boldsymbol{f_a}(\boldsymbol{V_E}, \boldsymbol{a}, \boldsymbol{u}, \Phi, \Theta, \lambda, \Omega) = \boldsymbol{0} \\ f_\lambda(\boldsymbol{V_E}, \boldsymbol{a}, \boldsymbol{u}, \Phi, \Theta, \lambda, \Omega) = 0 \\ Q_{mr}(\boldsymbol{V_E}, \boldsymbol{a}, \boldsymbol{u}, \Phi, \Theta, \lambda, \Omega) = 0 \end{cases}$$

The problem is a nonlinear system of 11 equations in 11 unknowns (10x10 considering $a_0 = cost$) and it has been solved using a Gradient method.

In Figure 1 is shown the steady descent rotational speed Ω as a function of the sink rate w_E and advanced velocity u_E while Figure 2 reports how sink rate and rotor speed vary as function of collective for fixed advancing speed. Here, fixing an advancing velocity u_E, sink rate and rotor angular rate decrease when high values of collective are chosen. This is because for the vertical equilibrium is $W \cong T$ and the thrust is approximately proportional to Ω^2, θ_0, w_e . A compromise needs to be found between w_E and Ω, where the first should be minimized and the second should be maximized.

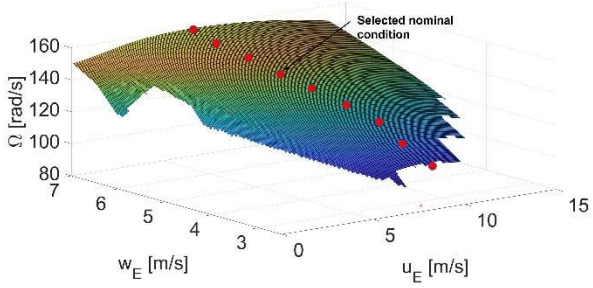

Figure 1: Rotor speed in autorotation steady descent

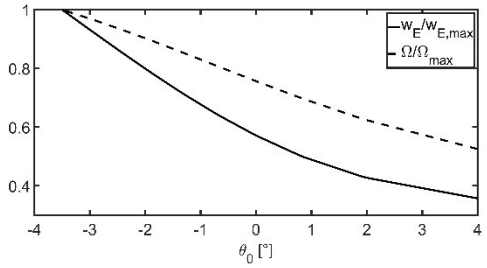

Figure 2: Sink rate and rotor angular rate as function of collective when a fixed $u_E = 7.5\ m/s$ is chosen.

Looking again at Figure 1 and moving on $w_E = cost$ curves, rotor speed has a maximum for advancing velocities around 7-9 m/s which correspond approximately to the condition of minimum power.

Red points in Figure 1 are obtained choosing the higher Ω for fixed values of w_E. A good choice, in the design of a suitable autorotation maneuver, is to pick steady descent conditions between these points.

2.2.2. Flare

The flare represents the most critical phase for autorotation. During the flare collective and longitudinal commands need to be managed in order to use rotor kinetic energy to reduce advancing and descent velocities at touch down. A critical issue is the evaluation of the proper altitude at which the flare should starts. An early flare can be catastrophic since the rotor energy and its capability of delivering a thrust can run out before touch down leaving the helicopter in a free fall. To the other side, a late flare hasn't the time necessary to decelerate the rotorcraft with a similar bad result.

The starting idea in modelling a suitable flare manoeuvre, is considering that during the flare both horizontal and vertical velocities have to reduce while the altitude reduces too. An exponential form is then hypothesized:

$$h^{id}(t) = h_{flare}\, e^{-\frac{t}{\tau_z}}$$
$$w_E^{id}(t) = w_0 e^{-\frac{t}{\tau_z}} \quad (25)$$
$$u_E^{id}(t) = u_0 e^{-\frac{t}{\tau_x}}$$

Where h_{flare} is the flare altitude, u_0 and w_0 are the initial conditions taken as the steady descent velocities and τ_z, τ_x are the exponential parameters which need to be chosen. Such a mathematical form has two important advantages:

- Ideally it is possible to obtain arbitrarily small velocity at arbitrarily small residual altitude if correct values of τ_z, τ_x are chosen. In practice we can obtain very small velocities at touch down.
- In simulation, the exponential desired trajectory can be easily evaluated in a closed loop logic. At every time step we can indeed calculate the desired velocity starting from the measured altitude as:

$$w_e^{id}(t) = -\frac{dh^{id}}{dt} = \frac{h_{flare}}{\tau_z}\, e^{-\frac{t}{\tau_z}} = \frac{h^{id}(t)}{\tau_z} \approx \frac{h(t)}{\tau_z}$$

$$u_e^{id}(t) \approx \frac{u_0}{h_{flare}} h^{id}(t) \approx \frac{u_0}{h_{flare}} h(t) \quad if\ \ \tau_x \approx \tau_z$$

Moreover, once the steady descent conditions are chosen, and the exponential parameters are correctly evaluated, it is possible to calculate the right value of the altitude for the flare as:

$$h_{flare} = w_0 \tau_z \quad (26)$$

2.3. Control system for autorotation

Different controllers have been designed for the different phases of autorotation. A first logic permits to recognize which control strategy needs to be adopted:

- When Ω decreases under a minimum value $\Omega_{decision}$ the system switches from the Engine ON control system to the autorotation control.
- When the altitude h is equal to h_{flare} a second logic is activated to perform the flare.

2.3.1. Pitch and roll stabilizer

A basic stabilizer logic is used in normal flight conditions. The scheme is reported in **Errore. L'origine riferimento non è stata trovata.**. In both cases, an inner loop controls pitch/roll rates while, in the outer loop a desired pitch/roll angle is compared with the actual attitude and the error generated becomes a reference for the inner loop. Finally, a sort of proportional mixing logic is added to reduce couplings between the two axes.

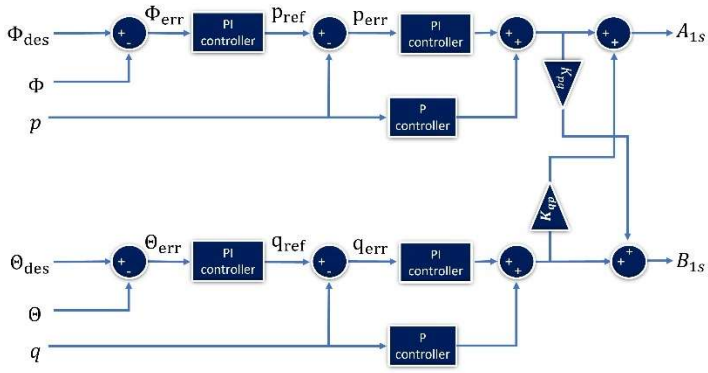

Figure 3: Roll and PItch Stabilizzer

2.3.2. Heading Hold Logic

The Heading Hold logic is shown in Figure 4. The desired yaw rate is compared with the actual yaw rate and the error is integrated to obtain an estimated yaw error. The latter is used to elaborate a desired yaw rate that again, compared with the actual yaw rate generates the error used to elaborate θ_{tr}. A fixed θ_{tr} is added to consider the tail rotor thrust needed to balance main rotor torque at hovering. Another contribution for θ_{tr} is finally proportional to θ_0 and takes into account how tail rotor thrust needs to modulate as a function of main rotor torque, and thus as a function of collective command.

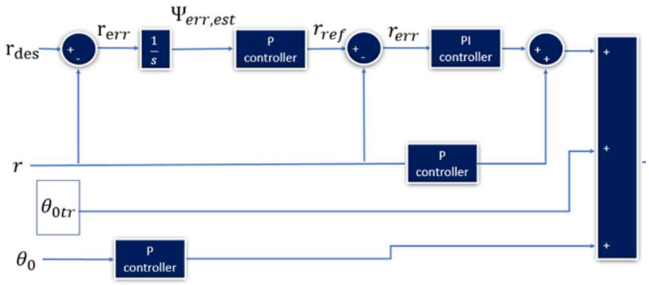

Figure 4: Heading hold

2.3.3. Steady descent control logic

For the steady descent, the strategy is to bring the system to the chosen steady state condition, namely Ω_{sd},$u_{E_{sd}}$,$w_{E_{sd}}$. This is done implementing a control on Ω and u_e as shown in Figure 5. Here, in the first phase, collective pitch is set to the nominal value $\theta_{0,sd}$.When rotor speed decreases under the nominal value, a PI feedback control on Ω elaborates the collective pitch θ_0 keeping $\Omega = \Omega_{sd}$. At the same time, the error between the desired velocity and the actual one $u_{E_{sd}} - u_E$ generates the reference Pitch angle given to the Pitch stabilizer to elaborate the longitudinal control B_{1s}. Similar control is done for A_{1s} where a desired zero lateral velocity v_E is used to elaborate a reference roll angle for the roll stabilizer. Finally, the tail is controlled by the heading hold, where θ_{tr0} is set to zero considering that thanks to the free-wheel mechanism the rotor torque is no more discharged to the fuselage in autorotation.

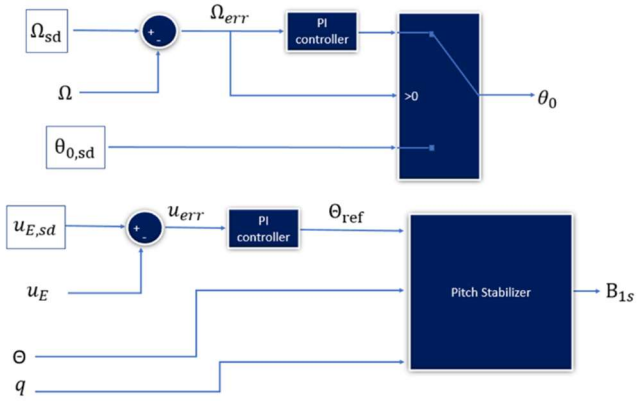

Figure 5: Steady descent control

2.3.4. Flare control system

The flare control logic is made up of two main modules: a trajectory planner, and a trajectory tracker. The first one evaluates, at every time step, a desired vertical and horizontal velocity proportional to the measured altitude, as shown in the previous sections. The tracker is an autopilot which evaluates the errors on velocities and calculates a reference attitude and a collective command. The desired attitude is given to the stabilizer which generates the cyclic commands.

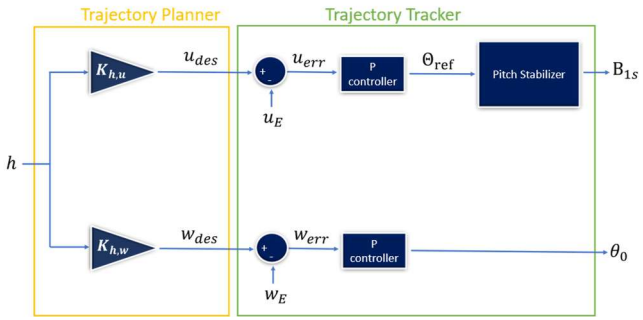

Figure 6: Flare control logic

3. SIMULATIONS

3.1.1. Simulations parameters

The complete autorotation landing has been simulated implementing the described model on Simulink. Main Helicopter parameters for the Goblin Saab 700 Helicopter used here, can be found in Tables 2-4. For all the simulations the following assumptions are considered:

- Infinite extended landing field and no constraints on final position
- Engine failure happens after $\mathbf{5}\boldsymbol{s}$ of stable level flight
- The control system recognizes the engine failure and starts the autorotation when $\boldsymbol{\Omega} < \boldsymbol{\Omega_{decision}}$ which is set to 95% of the value for normal flight
- Constraints for a safe autorotation landing are reported in equation (22).
- During autorotation, the control system brings the helicopter to the nominal steady descent condition reported in Table 1, and then perform the flare as described in previous sections.

3.2. Choice of a nominal maneuver

A preliminary step before the simulation campaign is the identification of a good nominal manoeuvre. First, steady descent conditions need to be chosen among the trim conditions founded in Section 2.2.1. The choice adopted here is reported in Table 1 and is located in the central region of Figure 1. However simulations shows that several different choices can be done. Once the steady descent condition are set, it is possible to evaluate good values of h_{flare}, τ_z, τ_x

which are all related as in equation 26.

During the flare a fairily fast and wide pull-up is made. The smaller the flare altitude, the more impulsive the maneuver. The criterion adopted here is to choose h_{flare} such that acceptable small touch down velocity is obtained, while pull-up angle is kept under 30°. In Figure 7 it is possible to see that such a result can be obtained for h_{flare} over 7.5 m which is choose as nominal value.

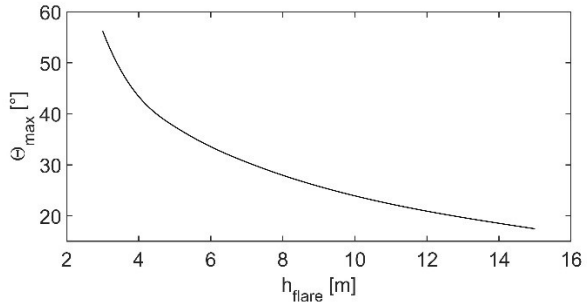

Figure 7: Maximum pitch angle during flare for nominal steady state conditions and varying h_{flare}

3.3. Results for nominal initial conditions

Nominal initial conditions are $\boldsymbol{h_0 = 200m}$ and $\boldsymbol{V_E 0 = [7.5\ 0\ 0]'\ m/s}$. We take the advancing velocity equal to the steady descent advancing velocity. Simulation results are reported in Figure 8. After the engine failure at 5s, the vertical velocity starts to increase while the rotor speed decreases. An instant yaw displacement appears since the system need few instants to recognize the failure and starts the autorotation (the condition is $\Omega < \Omega_{decision}$). The rotorcraft is then brought to nominal steady descent conditions ($\boldsymbol{\Omega = 142\ rad/s\ ; w_E = 5.5\ m/s}$). When $\boldsymbol{h_{flare} = 7.5\ m}$ is reached, the collective starts to increase while a doublet on the pitch command gives a quite fast and wide positive pitch maneuver. At touch down sink rate and advancing speed are reduced under the acceptable threshold, as for Euler angles. In Figure 9 it is possible to see how, during the flare, the desired exponential trajectory for the velocities, which is calculated by the trajectory planner, is tracked by the control system.

3.4. Behaviour for different velocities

Three simulations at different initial velocity have been performed. Results are shown in Figure 10: In all the cases the helicopter performs the steady descent and the flare in a good way, reaching acceptable touch-down velocities and attitude. We can here notice that, when u_{sd} is higher than the initial advancing velocity, the system accelerates to reach the steady descent condition, and decelerate during the flare. This is not the best strategy, and such a case should be avoided, considering a new steady state condition. Anyway, the simulation gives a good landing, showing the robustness of the approach adopted. It also suggests that a next step could be the implementation of a system based on just few pre-designed nominal maneuver among which, the control system should choose the one with steady descent conditions closest to the initial conditions.

3.5. Behaviour for different altitudes

The influence of the initial altitude on the success of the designed autorotation maneuver is investigate simulating three different initial altitudes and the nominal initial velocity. Results are plot in Figure 11. What happens is that, for $\boldsymbol{h_0 = 200m}$, steady descent and flare are regularly performed, while reducing the initial altitude the time for steady descent reduces since, for $\boldsymbol{h_0 = 10m}$,the altitude is already almost adequate to just perform the flare. All the simulation gives acceptable autorotation landing.

4. CONCLUSIONS

This paper presented the design of an automatic autorotation maneuver for a small-scale unmanned helicopter. The maneuver is divided in two main phases: a steady descent, and a flare. Helicopter dynamics was modelled by means of a 10 DOF nonlinear system. All the possible steady descent conditions have been calculated solving an algebraic system by means of an iteratively method. What results is that high values of rotor speed, require low values of collective pitch, driving to high rate of descent as well as high inflow, necessary for the wind-mill state. Thus, during the steady descent a trade-off between the sink rate (which should be limited) and the rotor speed is a mandatory task. For the flare, a decreasing exponential form for horizontal and vertical velocities has been selected as ideal trajectory. Main advantage of this choice is the simplicity in the implementation of a closed loop control logic able to generate the ideal trajectory starting from the measured altitude, at every time step, and to track it by means of autopilots.

A nominal maneuver (nominal steady descent, nominal h_{flare} and flare profile) and different initial conditions (altitude and level flight velocity) have been considered in simulation. Results show that for all the cases, the system recognizes the engine failure and performs the autorotation bringing the helicopter to steady descent conditions and later performing the flare when $h < h_{flare}$. Final velocities and attitude are all under the thresholds of equation (22). Robustness with respects to different initial conditions shows that, in the horizon of an

autonomous autorotation system, one strategy could be to Implement a system where, as a function of the initial conditions, the system choose among few pre-designed autorotation patterns, selecting the one having steady descent conditions closest to the initial advancing velocity at failure.

Nominal steady descent conditions		
$u_{E,sd}$	7,5	m/s
$w_{E,sd}$	5,5	m/s
Ω_{sd}	142	rad/s
Φ_{sd}	0,01	°
Θ_{sd}	3,73	°
$\theta_{0,sd}$	−1,89	°
Flare profile parameters		
h_{flare}	7,5	m
τ_z	0,734	
τ_x	1	

Table 1: Designed nominal maneuver parameters

Parameters		**Value**	**Unit**
Total mass	M_{tot}	4.8	kg
Inertia moments	I_{xx}	0.0465	$kg \cdot m^2$
	I_{yy}	0.2971	$kg \cdot m^2$
	I_{zz}	0.2567	$kg \cdot m^2$
Inertia products	I_{xy}	0.0079	$kg \cdot m^2$
	I_{xz}	0.0033	$kg \cdot m^2$
	I_{yz}	−0.0006	$kg \cdot m^2$

Table 2: Mass and Inertia parameters for Goblin Saab 700 Helicopter

Parameters		**Value**	**Unit**
Tail Rotor speed in normal flight	$\Omega_{tr,100\%}$	1447	$\frac{rad}{s}$
Tail Rotor Radius	R_{tr}	0.115	m
Number of blades	$N_{b_{tr}}$	2	$--$
Tail Rotor solidity	σ_{tr}	0.1716	$--$
Tail rotor position in body axes	$r_{tr} = \begin{bmatrix} x_h \\ y_h \\ z_h \end{bmatrix}$	$\begin{bmatrix} -1.045 \\ 0.052 \\ -0.031 \end{bmatrix}$	m

Table 3: Tail rotor parameters for Goblin Saab 700 Helicopter

Parameters		**Value**	**Unit**
Rotation direction	χ	$-1\ Clockwise$	$--$
Rotor speed in normal flight	$\Omega_{100\%}$	208	$\frac{rad}{s}$
Radius	R	0.79	m
Rotational Inertia	I_{mr}	0.0689	$kg \cdot m^2$
Number of blades	N_b	2	$--$
Virtual Hinge Offset ratio	ε	0.0314	$--$
Airfoil lift slope	Cl_α	2π	$1/rad$
Airfoil chord	c	0.06	m
Blade mass	m_b	0.2057	kg
Blade inertia about flapping hinge	I_b	0.0344	$kg \cdot m^2$
Flapping stiffness	K_β	162.69	$N \cdot m/rad$
Pitch-Flap coupling	K_1	0	$--$
Blade twist	θ_t	0	rad/m
Rotor solidity	σ	0.0479	$--$
Rotor shaft tilt angle	i_s	0.0524	rad
Precone	a_0	0	rad
Hub position in body axes	$r_h = \begin{bmatrix} x_h \\ y_h \\ z_h \end{bmatrix}$	$\begin{bmatrix} 0.0095 \\ 0 \\ -0.1810 \end{bmatrix}$	m

Table 4: Main rotor parameters for Goblin Saab 700 Helicopter

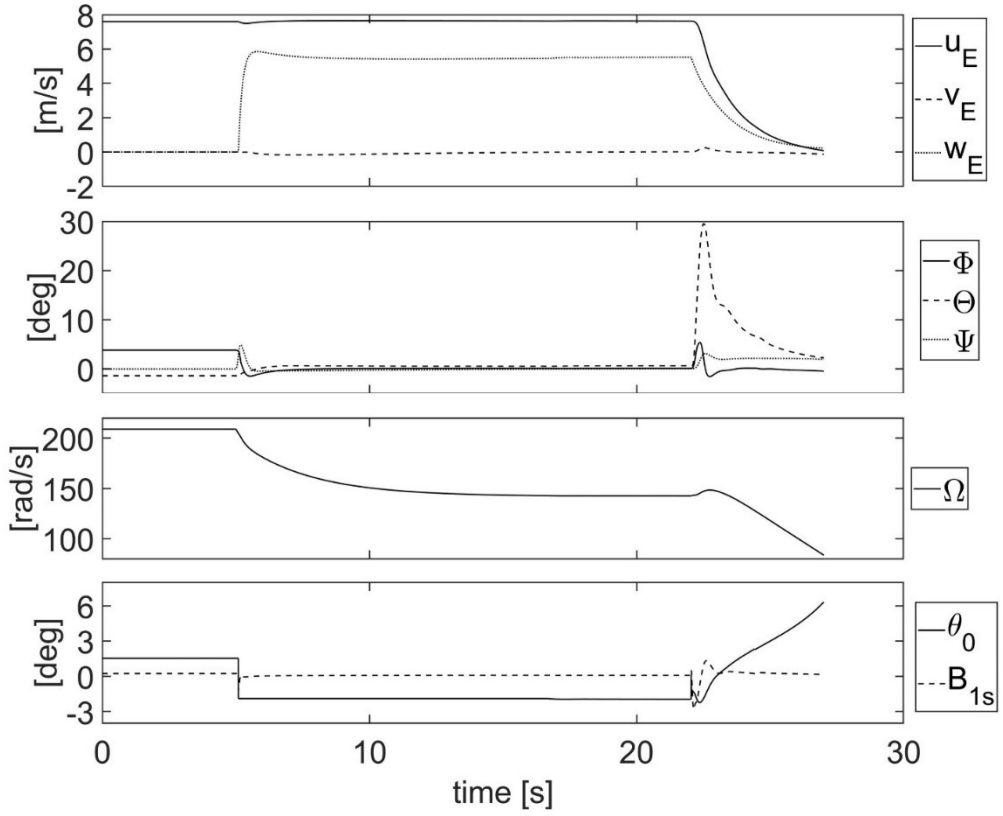

Figure 8: Simulation results for $h_0 = 200m$ and $u_{E0} = 7.5m/s$

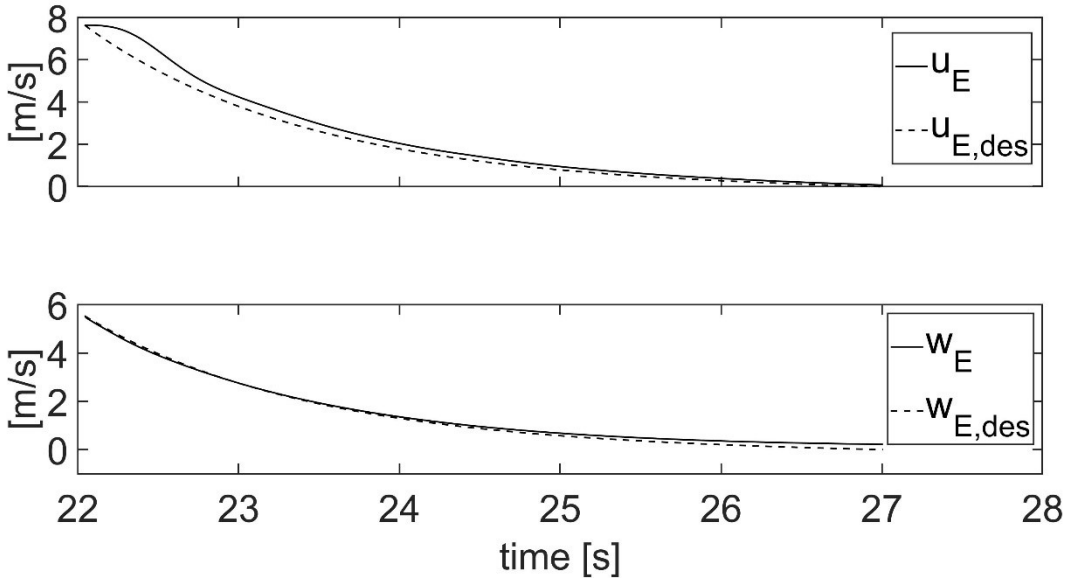

Figure 9: Tracking of the desired velocities during flare in nominal maneuver

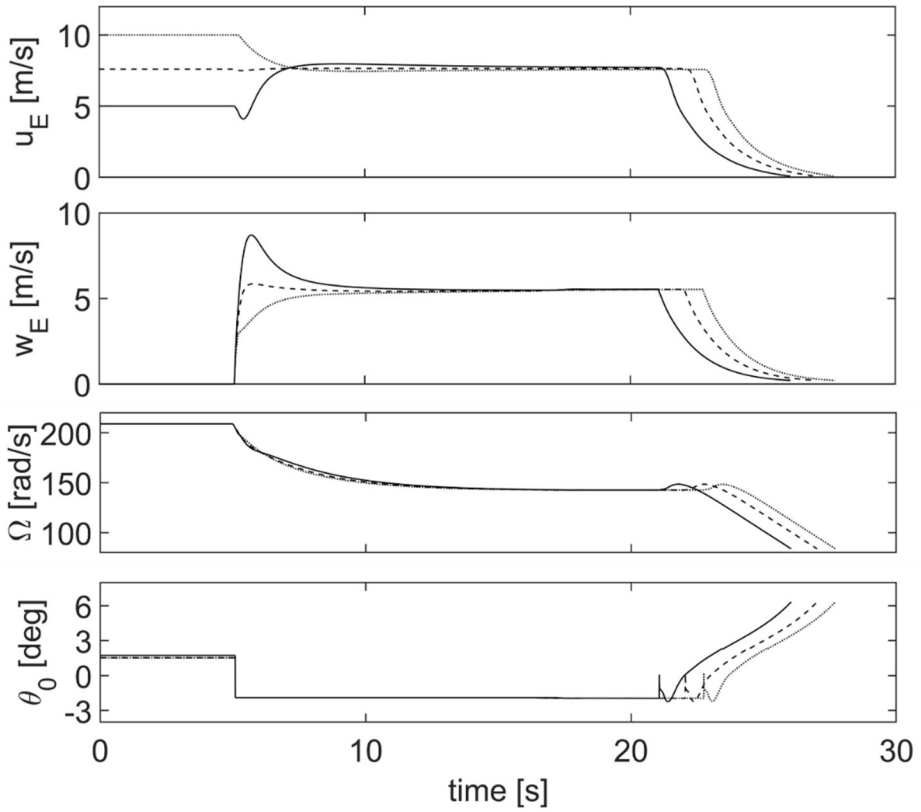

Figure 10: Simulation results for different initial velocities ($— 5\frac{m}{s}$; $-- 7.5\ \frac{m}{s}$; $\cdots 10\frac{m}{s}$) *and* $h_0 = 200m$

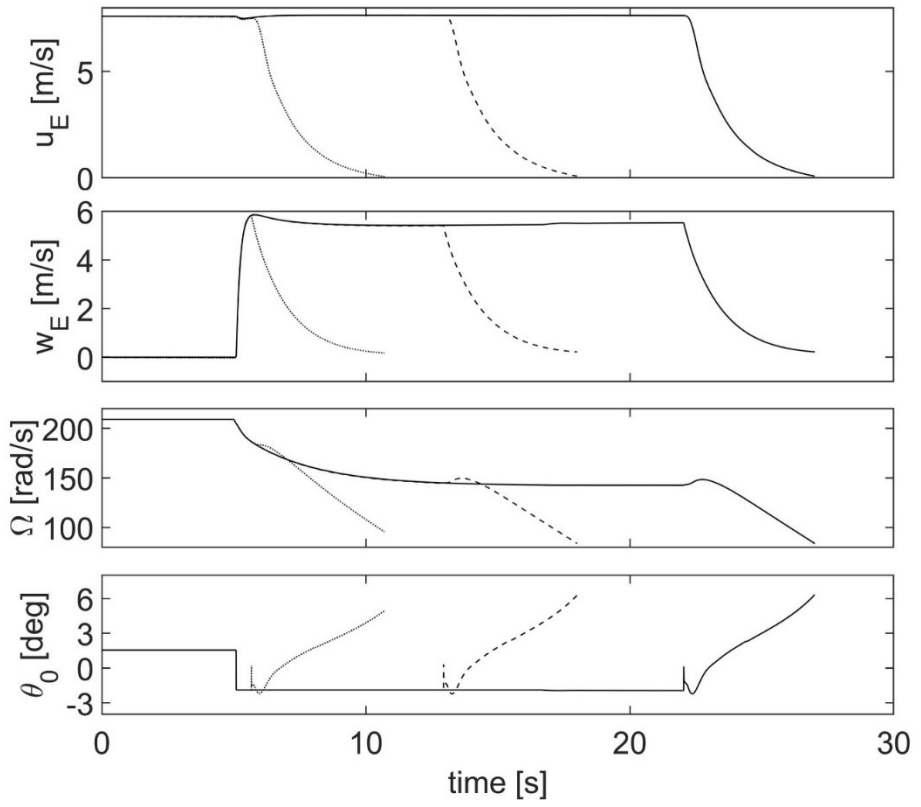

Figure 11: Simulation results for different initial altitudes ($—200m$; $-- 50m$; $\cdots 10m$) *and* $u_{E0} = 7.5\ m/s$

REFERENCES

[1] W. Johnson, «Helicopter optimal descent and landing after power loss,» May 1977.

[2] P. Bibik e J. Narkiewicz, «Helicopter Optimal Control After Power Failure Using Comprehensive Dynamic Model,» *Journal Of Guidance, Control, ans Dynamics,* vol. 35, n. 4, pp. 1354-1362, July–August 2012.

[3] S. Taamallaha, X. Bomboisb e P. M. Van den Hofc, «Trajectory planning and trajectory tracking for a small-scale helicopter in autorotation,» *Control Engineering Practice,* n. 58, p. 88–106, 2017.

[4] R. T. N. Chen, «Effects of primary rotor parameters on Flapping Dynamics,» *NASA Technical Paper 1431,* January 1980.

[5] D. Peters e N. HaQuang, «Dynamic Inflow for practical applications,» *Journal of American Helicopter Society TN,* October 1988.

[6] R. T. N. Chen, «A simplified rotor system mathematical model for piloted flight dynamics simulation,» Ames Reaserach Center, NASA, Moffett Field, California, May 1979.

[7] P. D. Talbot, B. E. Tinling, W. A. Decker e R. T. N. Chen, «A mathematical model for a single main rotor helicopter for piloted simulation,» Ames Reasearch Center, Moffett, Field, California, September 1982.